

Article

Phenazine Based Donor Acceptor Systems as Organic Photocatalysts for 'Metal-Free' C-N/C-C Cross Coupling

Harnimarta Deol, Gurpreet Singh, Manoj Kumar, and Vandana Bhalla

J. Org. Chem., **Just Accepted Manuscript** • DOI: 10.1021/acs.joc.9b03407 • Publication Date (Web): 23 Jul 2020

Downloaded from pubs.acs.org on July 23, 2020

Just Accepted

"Just Accepted" manuscripts have been peer-reviewed and accepted for publication. They are posted online prior to technical editing, formatting for publication and author proofing. The American Chemical Society provides "Just Accepted" as a service to the research community to expedite the dissemination of scientific material as soon as possible after acceptance. "Just Accepted" manuscripts appear in full in PDF format accompanied by an HTML abstract. "Just Accepted" manuscripts have been fully peer reviewed, but should not be considered the official version of record. They are citable by the Digital Object Identifier (DOI®). "Just Accepted" is an optional service offered to authors. Therefore, the "Just Accepted" Web site may not include all articles that will be published in the journal. After a manuscript is technically edited and formatted, it will be removed from the "Just Accepted" Web site and published as an ASAP article. Note that technical editing may introduce minor changes to the manuscript text and/or graphics which could affect content, and all legal disclaimers and ethical guidelines that apply to the journal pertain. ACS cannot be held responsible for errors or consequences arising from the use of information contained in these "Just Accepted" manuscripts.

Phenazine Based Donor Acceptor Systems as Organic Photocatalysts for ‘Metal-Free’ C-N/C-C Cross Coupling

*Harnimarta Deol, Gurpreet Singh, Manoj Kumar and Vandana Bhalla**

Department of Chemistry, UGC Centre of Advanced Study

Guru Nanak Dev University, Amritsar 143005, and Punjab, India

KEYWORDS: *C-N coupling, donor acceptor system, photoredox, reduction potential, Sonogashira Coupling.*

ABSTRACT: With an aim to achieve a balance between ground state and excited state reduction potential of donor acceptor systems for efficient C-N/C-C cross coupling, a series of donor acceptor systems **DA1-DA4** have been synthesized by varying the donor strength and connecting positions. With an increase in donor strength, systematic elevation in the ground state reduction potential and decrease in HOMO-LUMO gap was observed. Interestingly, all the derivatives **DA1-DA4** could catalyze C-N bond formation reaction between activated aryl halides and amines at low catalytic loading under metal-free conditions

without need of any external base upon irradiation with white LED. A balance was realized in case of derivative **DA2** which exhibits high efficiency in C-N couplings. Different control experiments support the validity of the energy as well as electron transfer pathways in the visible light mediated C-N bond formation. This study further reveals the potential of derivative **DA1** in 'metal free' Sonogashira coupling involving activated aryl halides which is attributed to its high excited state reduction potential.

1. INTRODUCTION

The C-N/C-C bond formation via palladium catalyzed coupling reaction is an introductory method to access complex architectures of natural, pharmaceutical and functional materials.¹⁻⁵ Unfortunately, wide spread use of palladium based catalytic systems is hampered by a few reaction elements such as high cost/toxic nature/sensitive handling of palladium, need for high equivalents of base and high reaction temperature.^{6,7} The pursuit for alternate 'green' catalytic systems for efficient and ecofriendly aminations of aryl halides encouraged the researchers to design copper based catalytic platforms. Over the years, a variety of copper based catalytic systems for Ullmann type coupling reaction have been developed which have undergone tremendous improvisation to construct C-N bond under controlled

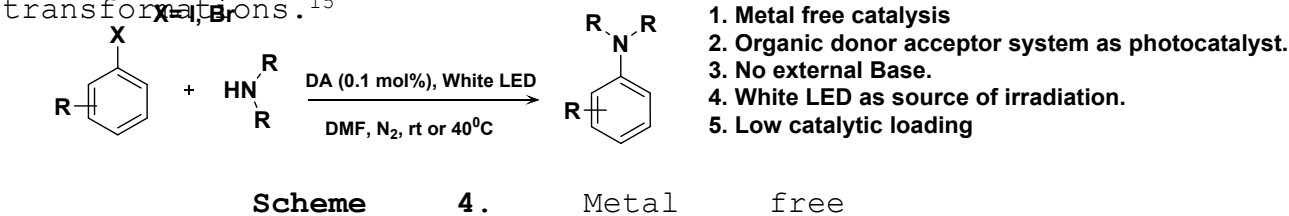
thermal conditions (100 °C).^{8,9} To get rid of thermal heating, photoinduced C-N bond formation has been reported in which Cu-amine complex facilitated the aryl amination through single electron transfer (SET) under photocatalytic conditions. However, the reaction conditions require the presence of high

energy UV radiation as energy source.¹⁰ Building on pioneering photocatalytic C-N arylation via electron transfer processes, Ni based photocatalytic systems have been developed by integrating nickel complex with different photocatalysts for C-N

bond formation with a good substrate scope (Scheme 1).¹¹⁻¹³ Very recently a nickel based catalytic system has been reported which catalyzed C-N coupling through energy transfer pathway and works efficiently with electron deficient aryl halides and secondary amine.¹⁴ Despite the environmental benefits, the nickel centered

photoredox system could not attain the target of sustainable chemical process due to use of organic bases, blue LED as irradiation source and high cost of iridium salts. To overcome some of these limitations 'photocatalyst free' nickel centered catalytic system has been developed (Scheme 2) but high energy

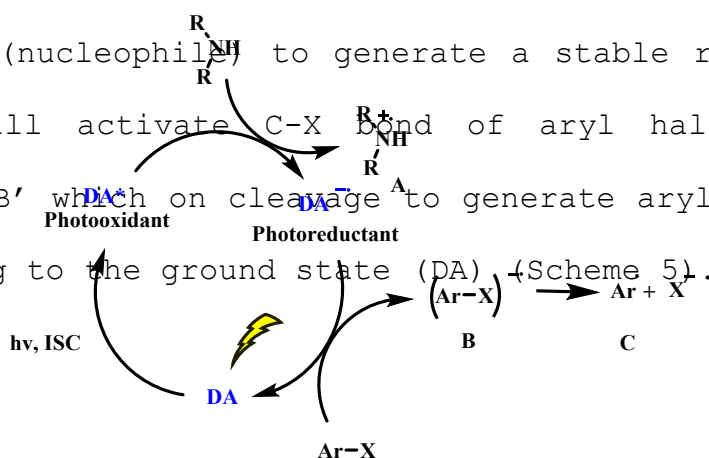
source (blue LED) was still needed to catalyze the transformations.¹⁵



Encouraged by economical and sustainable advantages of pure organic photocatalysts in organic transformations, very recently a 'metal free' organic semiconductor mesoporous carbon nitride (mpg-CN) material has been reported which catalyzes C-C/C-N bond formation through oxidative and reductive electron transfer processes (Scheme 3).¹⁶ Though mpg-CN could catalyze the formation of C-C bond under 'metal free' conditions but for construction of C-N bond, the assistance of Ni-complex was

needed. Thus, it is still a challenge to prepare pure organic photoredox catalyst for efficient formation of C-N bond under 'metal free' conditions.

Our interest in the development of organic photocatalytic systems motivated us to develop 'metal free' photoredox systems for C-N bond formation.¹⁷ For convenient C-N bond formation, activation of substrate *i.e.* aryl halide and nucleophile (amine) is vital. We visualized a catalytic cycle for C-N bond formation reaction involving organic photocatalyst^{18,19} (Scheme 5) which is analogous to that of metal based photoredox catalysts.^{11,16} As per hypothesized mechanism, upon excitation the organic photocatalyst (DA*) will undergo reduction in the presence of electron donor (nucleophile) to generate a stable radical anion (DA^{•-}) which will activate C-X bond of aryl halide to form radical anion 'B' which on cleavage to generate aryl radical 'C' before returning to the ground state (DA) (Scheme 5).



Scheme 5. The proposed electron transfer process for 'metal free' C-N coupling under visible light irradiation.

For successful realization of the proposed mechanistic pathway, the designed organic photoredox catalytic system should have (i) high absorption in the visible region to ensure requirement of low catalytic loading in the organic transformations, (ii) high excited state reduction potential to easily accept the electron from amine in the excited state, (iii) sufficient ground state potential to activate aryl halide for the generation of aryl radical, (iv) effective intersystem crossing (ISC) and reverse intersystem crossing (RISC) for maximum transfer of the absorbed photons to excited state.^{20,21}

For preparing materials having high absorption in the visible region and sufficient redox potential, donor-acceptor (**DA**) platform showing ICT state are the best. In literature, a variety of photocatalysts having either high excited state or high ground state redox potential have been reported, however, there are few reports available regarding organic materials having sufficient excited state as well as ground state redox potential.^{20,21} Generally, materials having high ground state redox potential have low excited state redox potential and the other way round, however, for efficient C-N bond construction, a balance between excited state and ground state reduction potential of organocatalyst should be maintained. The donor acceptor system having strong donor groups usually have high ground state reduction potential and by directly connecting the

donor group to acceptor unit (without spacer) ground state reduction potential is further enhanced with decrease in HOMO-LUMO gap. We envisaged that by appropriate choice of donor units and by controlling the conformation of the **DA** system a balance between ground state and excited state reduction potential may be realized. For acceptor unit, we chose dibenzo[a, c] phenazine (DBPZ) derivative due to its known light harvesting^{22,23} and efficient ISC-RISC.^{24,25} To understand the structure-activity relationship for achieving balanced reduction potential in excited and ground state, we planned to examine the catalytic potential of **DA** systems having different donor groups (variable strength) with different connectivity (through spacer or direct) in C-N coupling reactions. To begin with, we planned to couple DBPZ core with anisole group and envisaged that resulting donor acceptor system **DA1** may exhibit ICT characteristics. Further, by connecting carbazole unit directly to DBPZ core through *N* arylation, we expect derivative **DA2** to show twisted conformation. As a test of our hypothesis, we carried out computational studies of derivatives **DA1** and **DA2**. In derivative **DA1** overlapping between HOMO-LUMO orbitals was observed whereas well separated HOMO-LUMO orbitals with twist angle of 66° were observed (*vide infra*) in case of derivative **DA2**. After carrying out DFT studies for derivatives **DA1** and **DA2**, we synthesized donor acceptor systems **DA1** and **DA2**, and to examine the effect of

donor strength on the catalytic efficiency, we also prepared derivatives **DA3** and **DA4** having relatively stronger donor units. As indicated by computational studies, the derivative **DA1** has ICT state whereas presence of TICT state was found in case of derivatives **DA2-DA4**. Furthermore, all the derivatives exhibit strong absorption in the visible region and systematically elevated reductive potential (-1.25 to -1.71 V) with a gradual decrease in their HOMO-LUMO gap upon increasing the donor strength. Interestingly, C-N coupling between 1-iodo-4-nitrobenzene and pyrrolidine progressed well using low loading (0.1 mol %) of pure organic photocatalysts and the desired product was obtained in excellent yield. To the best of our knowledge, this is the first report which demonstrates 'metal free' approach for carrying out successful C-N coupling under visible light using organic photocatalyst without using any external base (Scheme 4). In all the DPBZ derivatives, due to their low HOMO-LUMO gap low energy of light source (white LED) was sufficient for excitation and presence of base was not needed. Different control experiments support the validity of the energy as well as electron transfer pathways in the visible light mediated C-N bond formation. Among all the photocatalysts examined, **DA2** exhibits excellent efficiency towards amination of activated aryl halides (electron deficient) due to contribution of energy as well as electron transfer pathways. The derivative

DA1 fails to catalyze the organic transformations involving relatively less activated aryl halides such as 1-bromo-3,5-difluorobenzene and 4-bromobenzonitrile due to its insufficient ground state reduction potential. On the other hand, despite the highest ground state reduction potential, derivative **DA4** shows relatively poor catalytic activity due to its low excited state reduction potential. To sum up, a balance between ground and excited state potential was realized in case of derivative **DA2**. We also examined the catalytic efficiency of these photocatalysts in 'metal free' Sonogashira coupling in the presence of weak electron donor *i.e.* triethylamine. Though we were not disappointed by the weak catalytic activity of **DA2-DA4** under optimized conditions, we were delighted at good efficiency of **DA1** in Sonogashira coupling involving activated aryl halides as coupling partners. The high excited state reduction potential of **DA1** is the reason behind its good catalytic activity in Sonogashira coupling reaction.

2. RESULTS AND DISCUSSION

2.1 Synthesis and properties of DPBZ based donor acceptor systems.

The Suzuki Miyaura coupling between dibromo derivative of dibenzo [*a, c*] phenazine²⁶ **A1** and 4-methoxy phenyl boronic acid furnished the **DA1** in 80% yield (Chart 1) (Figures S70-72, SI).

Further, Ullman coupling between dibromo derivative of dibenzo [a, c] phenazine **A1** and different donors such as carbazole, 3,6-Di-*tert*-butyl-9H-carbazole and diphenylamine furnished DPBZ derivatives **DA2**, **DA3** and **DA4** in 70%, 70% and 80% yields, respectively (Chart 1) (Figures S73-S81, SI).

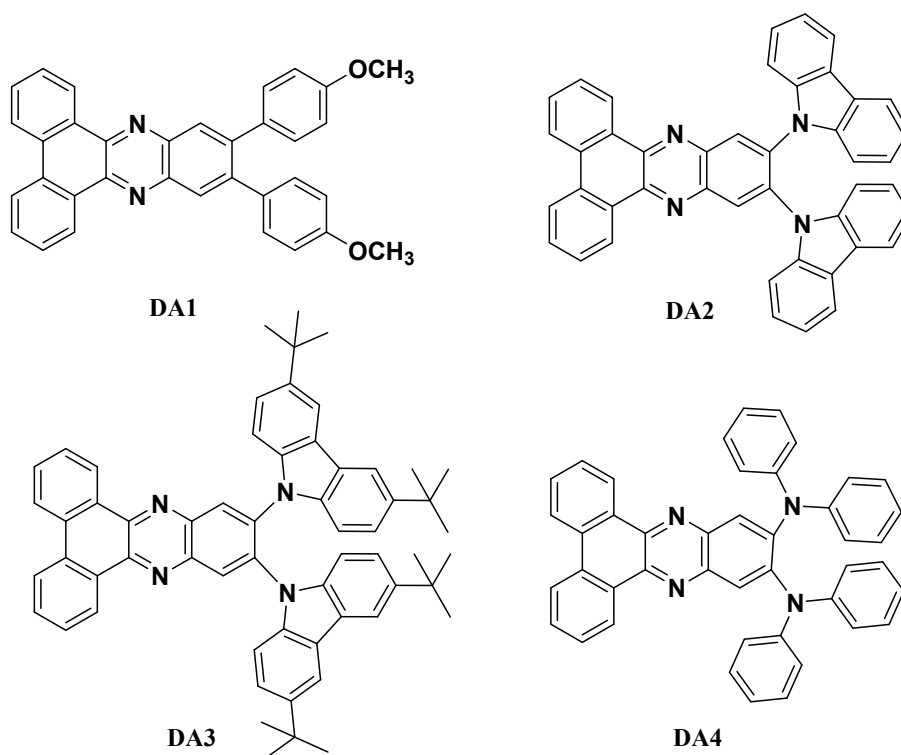


Chart 1. Molecular structure of donor acceptor

systems **DA1-DA4**. We carried out UV-vis studies of all the derivatives in DMF (Figure 1) and it was found that all the derivatives absorb strongly in the visible region due to intramolecular charge transfer (ICT) state (Table 1). Further, it was observed that ICT band is red shifted from 420 nm (**DA1**) to 470 nm (**DA4**) on changing the donor groups from anisole to diphenylamine. We also

carried out fluorescence studies of these derivatives in different solvents (non-polar to polar) and these studies confirm the existence of twisted intramolecular charge transfer state in case of derivatives **DA2-DA4** (Figures S1-S4, SI). Further, the emission band is red shifted from 510 nm to 605 nm on changing the donor groups from anisole to diphenylamine (Figure S5, SI). The quantum yields of all donor acceptor systems are given in table 1 and from these values it is clear that all the donor acceptor systems (**DA1-DA4**) are emissive in solution. The time resolved emission studies of derivatives **DA1-DA4** (Figures S6-S9, SI) show that **DA2** shows highest singlet excited state lifetime among all the derivatives (Table 1).

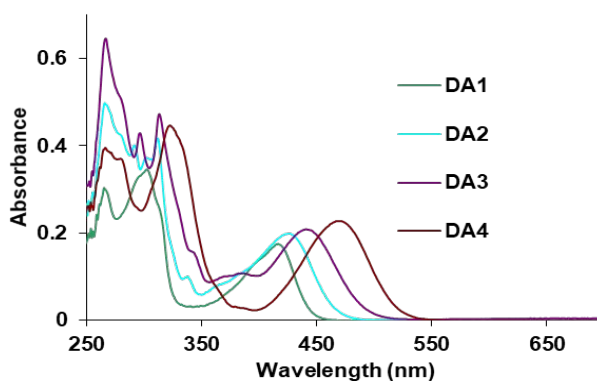


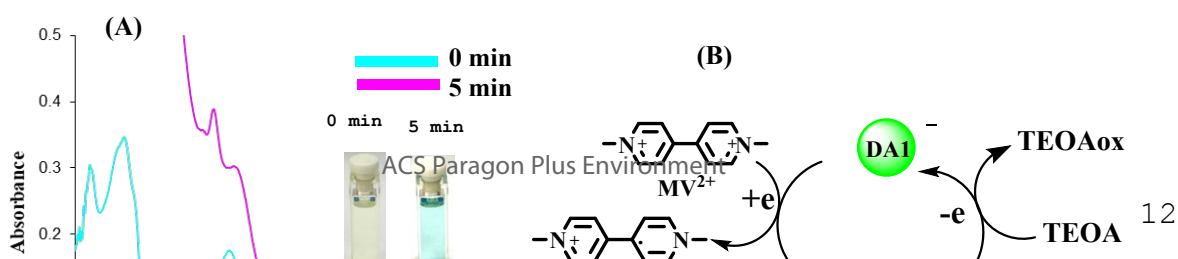
Figure 1. UV-vis spectra of **DA1** to **DA4**

Table 1. Photophysical properties of

Photocatalyst	Absorption maxima	Emission maxima	Quantum Yield	Singlet state lifetime	Reduction potential (V)	Calculated Excited state Reduction potential (V)	HOMO-LUMO gap (eV)
DA1	420 nm	510 nm	0.62	5 ns	-1.25, -0.88	1.55	2.8
DA2	426 nm	560 nm	0.38	8 ns	-1.49, -1.09	1.01	2.5

DA3	440 nm	595 nm	0.22	3.5 ns	-1.55, -1.23	0.90	2.3
DA4	470 nm	605 nm	0.32	3 ns	-1.71, -1.27	0.65	2.1

The DFT studies of derivative of **DA1** indicate the overlapping between its HOMO-LUMO molecular orbitals (Figures S10, SI) while DFT studies of derivatives **DA2-DA4** corroborate with their twisted geometry as is evident from the large dihedral angle between donor and acceptor units with complete spatial separation between HOMO-LUMO molecular orbitals (Figures S11-S13, SI). We observed that HOMO-LUMO gap reduced with increase in donor strength (Table 1). Further, the ground state reduction potential of all derivatives was evaluated by cyclic voltammetry studies in DMF using Ag/AgCl as reference electrode (Figures S14-S17, SI). The increase in the ground state reduction potential was observed with increase in the donor strength. Among all the derivatives, derivative **DA4** has highest reduction potential in ground state. Further, we calculated excited state reduction potential using Rehm Weller equation²⁷ and derivative **DA1** was found to have highest excited state reduction potential (Table 1). All the derivatives **DA1-DA4** show reversible reduction peaks which indicates high stability of their corresponding radical anion.¹⁹ The formation of stable radical anion is vital for smooth completion of the catalytic cycle.



Next, we checked the validity of our proposed mechanistic hypothesis *i.e* ability of **DA1-DA4** to act as photooxidants in the excited state and photoreductant in the ground state. We chose three component system in which triethanolamine (TEOA) as sacrificial donor, methyl viologen (MV^{2+}) as acceptor and donor acceptor systems (DA) as electron transporter. We examined the electron transfer from triethanolamine to methyl viologen (MV^{2+}) using donor acceptor system as transporters. We begin with **DA1** system and the solution containing methyl viologen (MV^{2+}), **DA1** and TEOA was exposed to visible light radiations under inert atmosphere. Within 5 min colour of the solution changed from colorless to

greenish blue. The whole event was also followed by UV-vis spectroscopy.

The UV-vis spectrum of the irradiated sample containing methyl viologen, **DA1** and TEOA exhibits presence of two new bands at $\lambda = 395$ and 603 nm corresponding to the reduced species $MV^{\bullet+}$ of methyl viologen (Figure 2A). We believe that derivative **DA1*** was reductively quenched by sacrificial donor in the excited state to generate **DA1⁻** which eventually reduces MV^{2+} to $MV^{\bullet+}$ (Figure 2B).²⁸⁻³⁰ Similar behaviour was observed when the same experiment was repeated with other donor acceptor systems (**DA2-DA4**) (Figures S18-S20, SI).

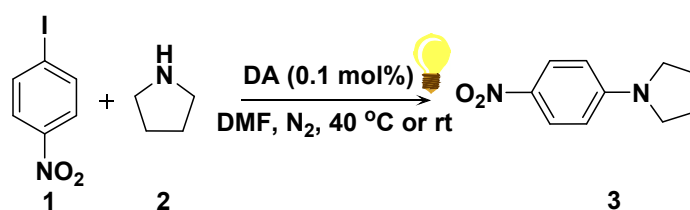
2.2 Metal Free C-N Cross Coupling.

After completing the initial monitoring, we examined the test reaction between 1-iodo-4-nitrobenzene (1 equiv.) and pyrrolidine (5 equiv.) in DMF under irradiation of white LED (16 W), at room temperature and under inert atmosphere using photocatalyst **DA1**. To our pleasure, the reaction was complete in 7 h and the desired product was obtained in 68% yield (Table 2, entry 1). To facilitate the reaction kinetics of model reaction catalyzed by **DA1**, we increased the temperature of model reaction mixture to $40\text{ }^{\circ}\text{C}$. The kinetics was accelerated and product formation was observed within 15 min (monitored by TLC) and a notable enhancement in the yield of target product was observed (92%) (Table 2, entry 2). Further increase in temperature did

not affect the yield significantly (Table 2, entry 3). Interestingly, the control reaction carried out under optimized conditions without any photocatalyst furnished the final product in 35% yield after 12 h (Table 2, entry 4) (*vide infra*). We repeated the model reaction without any photocatalyst and after 6 h when spot corresponding to product appeared on TLC, we removed the light source for next 6 h, however, the reaction did not proceed further (Table 2, entry 5). This study proves that continuous irradiation of light is necessary as no photocatalytically active species is generated in dark to further proceed the reaction. Further, to understand the importance of continuous irradiation of visible light, we repeated the model reaction under above mentioned conditions using **DA1** as photocatalyst. The reaction proceeds and after 4 h significant amount of product was formed (monitored by TLC), thereafter, we removed the light source for next 4 h, but no significant increase in the yield of product was observed during this time (monitored by TLC) (Table 2, entry 6). These studies prove the role of continuous irradiation of reaction mixture with light to achieve the target product in good yield. The model reaction when repeated under dark did not proceed (Table 2, entry 7). We also carried out EDX studies of **DA1** system but no palladium content was found. These studies clearly rule out the possibility of traces of palladium in **DA1** system to act as

catalyst (Figure 21, SI). Next, we examined the influence of number of equivalents of the amine substrate on reaction kinetics/yield. The model reaction using 3 equiv. of pyrrolidine shows a significant decrease in the yield of the target product (Table 2, entry 8). Thus, besides acting as one of the coupling partners, the amine substrate also acts as a sacrificial donor. Next, we screened different solvents such as toluene, ACN, THF, DMSO and glycerol as reaction media (Table 2, entries 9–13). The highest yield was obtained in case of DMF as solvent (Table 2, entry 2). We carried out several control reactions to examine influence of the presence/absence as well as nature of base on reaction outcome (Table 2, entries 14–16). Interestingly, the presence and absence of base had insignificant effect on the kinetics/yield of test reaction.

Table 2. Optimization of reactions conditions for



Entry	Photocatalyst	solvent	Base	Temp.	Time	Yield%
1.	DA1	DMF	-	rt	7 h	68%
2.	DA1	DMF	-	40 °C	3 h	92%
3.	DA1	DMF	-	60 °C	3 h	95%

4.	-	DMF	-	40 °C	12 h	35%
5.	-	DMF	-	40 °C	12 h	20% ^a
6.	DA1	DMF	-	rt	8 h	46% ^b
7.	DA1	DMF	-	rt	3 h	traces ^c
8.	DA1	DMF	-	40 °C	3 h	65% ^d
9.	DA1	Toluene	-	40 °C	3 h	80%
10.	DA1	ACN	-	40 °C	3 h	70%
11.	DA1	THF	-	40 °C	3 h	68%
12.	DA1	DMSO	-	40 °C	3 h	78%
13.	DA1	Glycerol	-	40 °C	3 h	70%
14.	DA1	DMF	K ₂ CO ₃	40 °C	3 h	90%
15.	DA1	DMF	<i>t</i> -BuOK	40 °C	3 h	92%
16.	DA1	DMF	DABCO	40 °C	3 h	93%
17.	DA1	DMF	-	40 °C	3 h	20% ^e
18.	DA1	glycerol	-	40 °C	3 h	50% ^e
19.	DA2	DMF	-	40 °C	3 h	90%
20.	DA3	DMF	-	40 °C	3 h	82%
21.	DA4	DMF	-	40 °C	3 h	78%
a. switch on light for 6 h and switch off for next 6 h.; b. switch on light for 4 h and switch off for next 4 h; c. dark conditions; d. 3 equiv. of pyrrolidine; e. aerial conditions						

To understand the need of inert reaction atmosphere, we repeated the test reaction under aerial conditions, however, the yield of desired product reduced to 20% (Table 2, entry 17).

Surprisingly, only in case of glycerol as reaction media, the desired product was obtained in 50% yield under aerial conditions (Table 2, entry 18). We believe that in the presence of highly viscous glycerol the diffusion of oxygen is restricted. All these control experiments confirm the requirement of light source, inert atmosphere and photocatalyst to achieve the rapid formation of product in high yield. Further, we repeated the test reaction using the photocatalysts **DA2**, **DA3** and **DA4** (Table 2, entries 19-21). Among all the photocatalysts examined, the derivatives **DA1** and **DA2** furnished the target compound in excellent yield (Table 2, entries 2 and 19) and relatively lower yield of product was obtained when **DA4** was used as catalyst (Table 2, entry 21).

With optimized conditions in hand, we examined the substrate scope with regard to nucleophiles i.e. cyclic amines (secondary), aliphatic amines and aromatic amines (aniline). In all the cases, the reactions proceed conveniently and desired products were obtained in good to moderate yield (Table 3, entries 1-6). Out of morpholine and piperidine, piperidine substituted product was obtained in relatively higher yield in case of all the photocatalysts (Table 3, entry 1).

Further, the primary aliphatic amines such as dimethylamine and *n*-butylamine furnished the desired products in comparatively lower yields in case of photocatalysts **DA3** and **DA4** (Table 3,

Table 3. The C-N coupling between 1-iodo-4-nitrobenzene and different amines using photocatalyst **DA1-DA4** under optimized

entries 3 and 4). These studies show that reaction kinetics and yield is strongly dependent upon nucleophilic strength of the amine substrate.

Entry	Aryl Halide	Amine	Time	Product	Yield%			
					DA1	DA2	DA3	DA4
1.			3 h		91%	89%	84%	80%
2.			8 h		75%	72%	58%	55%
3.			5 h		82%	80%	65%	60%
4.			3 h		88%	85%	66%	60%
5.			3 h		90%	85%	75%	68%
6.			10 h		68%	60%	40%	30%

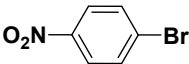
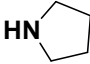
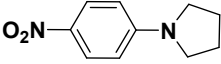
Next, we investigated the reaction of 1-iodo-4-nitrobenzene with ammonia using photocatalyst **DA1-DA4** (Table 3, entry 5). Again,

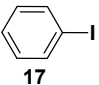
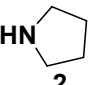
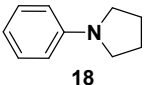
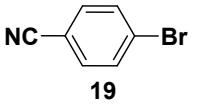
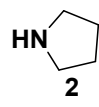
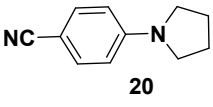
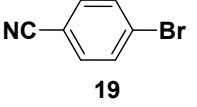
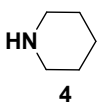
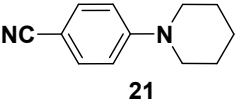
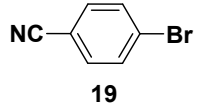
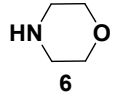
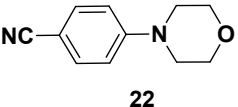
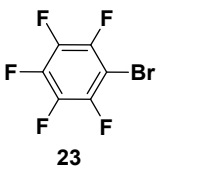
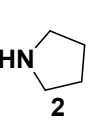
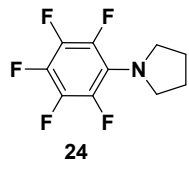
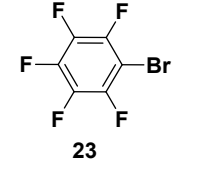
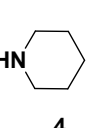
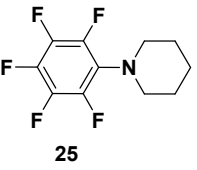
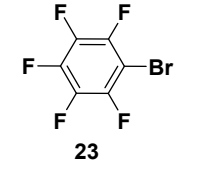
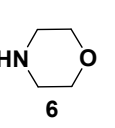
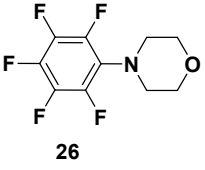
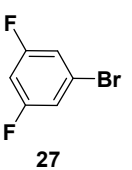
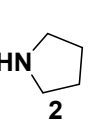
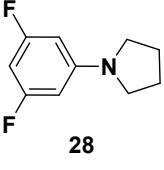
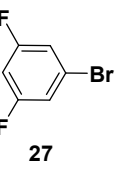
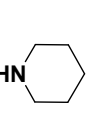
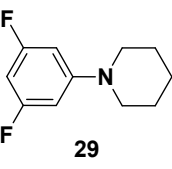
the derivatives **DA1** and **DA2** furnished target product in good yield, however, comparatively lower yield was obtained in case of derivatives **DA3** and **DA4**.

The C-N coupling between 1-iodo-4-nitrobenzene and aniline yields the desired product in 68% and 60% yield respectively in case of **DA1** and **DA2**, moderate yield (40%) in case of **DA3** and lower yield (30%) in case of **DA4** (Table 3, entry 6).

Next, we examined the effect of leaving group on the reaction kinetics. Interestingly, the coupling between 1-bromo-4-nitrobenzene with pyrrolidine progressed conveniently to furnish the target product in same yield and time as observed in case of 1-iodo-4-nitrobenzene using **DA1-DA4** as photocatalysts (Table 4, entry 1). We believe that due to the same reduction potential of 4-bromo/iodo-1-nitrobenzene derivative (-0.98 V),³¹ the rate of catalyst mediated

Table 4. The C-N coupling between electron withdrawing aryl halides and different amines using photocatalyst **DA1-DA4** under

Entry	Aryl Halide	Amine	Time	Product	Yield%			
					DA1	DA2	DA3	DA4
1.	 16	 2	3 h	 3	92%	90%	86%	80%

2.	 17	 2	24 h	 18	-	-	-	-
3.	 19	 2	12 h	 20	Traces	75%	65%	60%
4.	 19	 4	12 h	 21	Traces	72%	54%	50%
5.	 19	 6	12 h	 22	Traces	60%	50%	45%
6.	 23	 2	3 h	 24	93%	90%	85%	82%
7.	 23	 4	3 h	 25	90%	90%	82%	80%
8.	 23	 6	3 h	 26	82%	80%	70%	65%
9.	 27	 2	3 h	 28	Traces	82%	78%	74%
10.	 27	 4	3 h	 29	Traces	80%	70%	68%

11.			5 h		Traces	65%	58%	50%
-----	--	--	-----	--	--------	-----	-----	-----

substrate activation is same, thus, kinetics remained unaffected. Furthermore, the reaction between iodobenzene and pyrrolidine did not proceed under optimized conditions (Table 4, entry 2). We believe that due to high reduction potential of iodobenzene ($E_{\text{red}} > -2.1 \text{ V}$)^{32,33}, the ground state reduction potential of photocatalysts **DA1-DA4** is not sufficient to activate the C-X bond of aryl halide to generate aryl radical. To confirm this assumption, we examined several electron deficient aryl halides as coupling partners using photocatalysts **DA1-DA4** (Table 4, entries 3-11).

Upon replacing nitro group with nitrile, the photocatalysts **DA2-DA4** furnished the desired products in relatively lower yields (Table 4, entries 2-5), however, to our surprise, photocatalyst **DA1** failed to catalyze the transformation in case of 4-bromobenzonitrile as coupling partners. By using 1-bromopentafluorobenzene as reaction partner, the target products were attained in high yield (Table 4, entries 6-8), however, in case of 1-bromo-3,5-difluorobenzene the yields were affected and photocatalyst **DA1** again failed to catalyze the transformations (Table 4, entries 9-11).

To understand the mechanism of reaction, we begin with the control reaction between 1-iodo-4-nitrobenzene and pyrrolidine without using any photocatalyst under irradiation of visible light. The control experiment was repeated in the presence of 1 equiv. of TEMPO as radical scavenger. The reaction did not proceed and the mass spectrometric studies confirm the formation of TEMPO adduct (Figure S22, SI). This study supports the formation of aryl radical under reaction conditions (Scheme S6, SI). Further, we monitored the control reaction by absorption spectroscopy. The absorption spectrum of 1-iodo-4-nitrobenzene and pyrrolidine in DMF under inert atmosphere exhibits the formation of two bands at 500 nm and 600 nm which suggests the formation of electron donor acceptor (EDA) complex between 1-iodo-4-nitrobenzene (acceptor) and pyrrolidine (donor) in ground state^{34,35} (Figure S23, SI). The formation of EDA complex was visible to naked eye with clear change of color of the solution from colorless to light green. We believe that EDA complex is acting as light harvesting antenna and is catalyzing the reaction in the forward direction.

To understand the role of photocatalyst, we prepared EDA complex (between 1-iodo-4-nitrobenzene and pyrrolidine) and introduced it to solution of **DA1** system in DMF, complete quenching of the emission was observed in the fluorescence spectrum (Figure S24, SI) and a good spectral overlap between absorption spectrum of

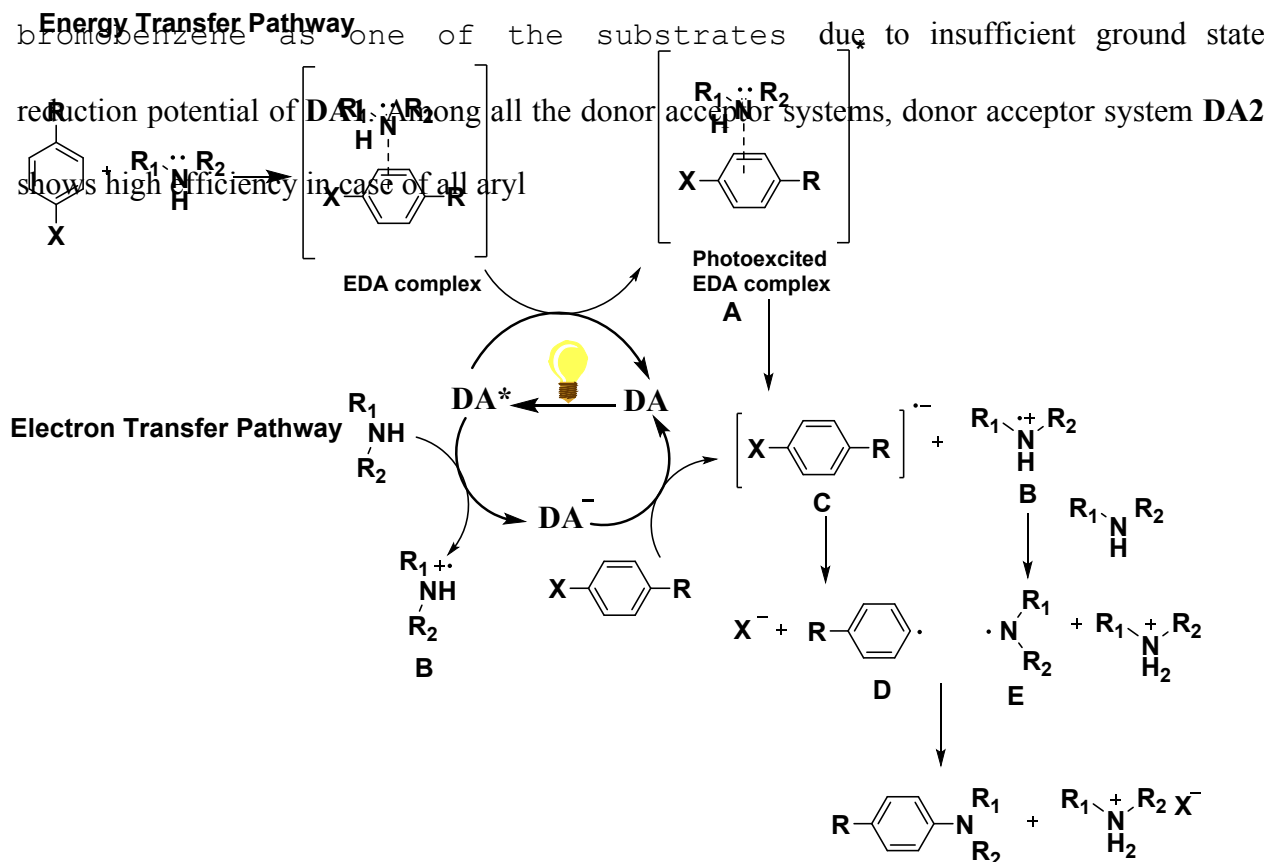
EDA complex and emission spectrum of **DA1** system was also observed (Figure S25, SI). These results indicate the possibility of energy transfer from **DA1** systems to EDA complex.¹⁴

Next, we also examined the fluorescence behaviour of donor acceptor system **DA1** (5 μ M, DMF) in the presence of pyrrolidine. Interestingly, in the presence of 10 equiv. of pyrrolidine, the derivative **DA1** shows quenching of the emission intensity (Figure S26, SI), however, no spectral overlap was observed between the emission of **DA1** system and absorption spectrum of pyrrolidine (Figure S27, SI). The quenching of emission may be attributed to photoinduced electron transfer (PET) from electron rich amine to **DA1** system^{36,37} which indicates the possibility of electron transfer pathway.

Similar behaviour was observed in case of **DA2** and **DA3** donor acceptor systems (Figures S28 and S31, SI) except in case of **DA4** (*vide infra*) (Figures S32 and S33, SI).

To get deep insight into the mechanistic pathway in case of other aryl halides, we examined the formation of EDA complex in case of 1-bromopentafluorobenzene, bromobenzonitrile and 3,5-difluoro bromobenzene using absorption spectroscopy (Figures S34-S36, SI). Among all, EDA complex was formed only in case of 1-bromopentafluorobenzene. These observations indicate that in case of relatively more electron deficient aryl halide (1-iodo-4-nitrobenzene and 1-bromopentafluorobenzene) reaction proceeds

through both electron as well as energy transfer pathways, however, in case of bromobenzonitrile, 3,5-difluoro bromobenzene the reaction proceeds through electron transfer pathway only. These results also clearly explain the inability of **DA1** to catalyze the reactions involving bromobenzonitrile, 3,5-difluoro



Scheme 6. The proposed energy transfer/electron transfer pathways for 'metal free' C-N coupling under visible light

halides which was due to more spectral overlap with absorption of EDA complex which enhances the rate through energy transfer pathway and the balanced reduction potential in excited and ground state enhances the rate of reaction through electron transfer pathway.

Further, we carried out model reaction in the presence of different equivalents of TEMPO using **DA1** as photocatalyst under optimized conditions. Upon introducing 0.5 equiv. of TEMPO to the reaction the yield of target product reduced to 30%, while upon introducing 1 equiv. of TEMPO, the progress of model reaction was inhibited and formation of TEMPO adduct was detected using mass spectrometric analysis (Figure S37, SI). These results indicate that energy transfer/electron transfer mechanistic route proceeds through the formation of radical intermediates (Scheme 6). In energy transfer pathway, **DA** system absorbs energy upon irradiation of visible light and transfers it to EDA complex. The photoexcited EDA complex 'A' complex then undergoes cleavage to form amino radical cation 'B' and aryl radical anion 'C', whereas, in case of electron transfer pathway, **DA** system absorbs visible light and is excited to form **DA*** (photooxidant) which then accepts electron from the amine to form radical anion **DA^{-•}** and amino radical cation 'B'. The radical anion **DA^{-•}** activates aryl halide by electron transfer to form anion radical 'C'. In both pathways, the radical anion 'C' undergoes cleavage to generate aryl radical D. On other hand, amino radical cation 'B' reacts with another molecule of amine

to form amino radical 'E'. Finally, aryl radical 'D' combines with amino radical 'E' to form the desired product.

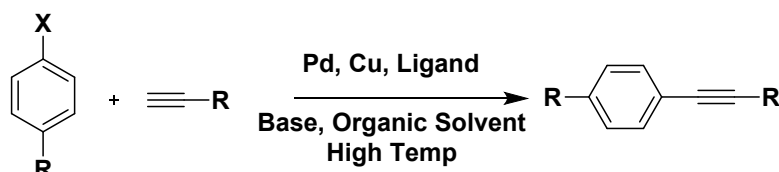
Another interesting observation in C-N coupling reaction is that the reaction kinetics depends on nucleophilic strength of amine. In case of strong nucleophile, the reaction proceeds at faster rate to furnish the target product in high yield.

The distinct photophysical behaviour of **DA4** in comparison to **DA1-DA3** in the presence of EDA complex and pyrrolidine suggests an alternative mechanistic pathway for completion of the reaction. To examine the possibility of oxidative quenching, we examined the emission behavior of **DA4** in the presence of 1-iodo-4-nitrobenzene. No change in the emission behavior was observed which rules out any possibility of oxidative quenching in the excited state (Figure S38, SI). However, different control experiments show that reaction kinetics is strongly dependent upon the number of equivalents of pyrrolidine (Figure S39, SI). Based on all the above experiments and literature reports, we believe that in case of **DA4**, ISC is efficient and the energy/electron transfer is operative through triplet state.³⁸

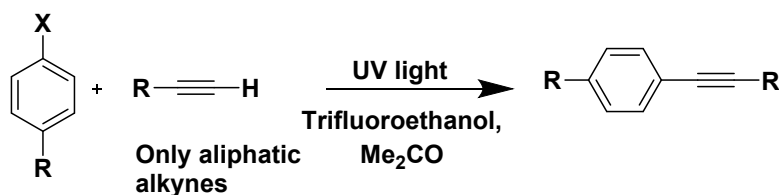
Furthermore, regardless of high molar extinction coefficient, lower HOMO-LUMO gap and high reduction potential in ground state, derivative **DA4** shows low catalytic activity in all the reactions. We believe that due to the presence of strong donor groups in **DA4**, electron density on acceptor part is high and hence its ability to accept the electron from the amine substrate upon excitation is reduced.³⁹ Moreover, the **DA4** has emission at longer wavelength (605 nm) due to which spectral overlap with EDA complex was decreased.

2.3 Metal Free Photocatalytic Sonogashira Coupling.

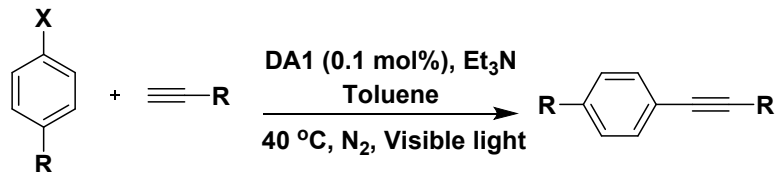
Classical Method ⁴⁰⁻⁴⁴



Metal Free Approach⁴⁵



Present Work

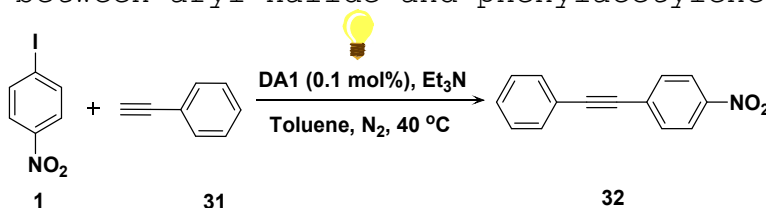


Scheme 7. Catalytic systems for

The ability of all the photocatalysts to accelerate aryl halides in ground state prompted us to examine their catalytic efficiency in Sonogashira coupling involving activated aryl halide and triethylamine (TEA) as electron donor due to its good basicity. To begin with, we chose the reaction between 1-iodo-4-nitrobenzene and phenylacetylene as model reaction using **DA1** as photocatalyst under optimized reaction conditions of C-N coupling. The desired product was obtained in 40% yield (Table 5, entry 1). Upon switching the solvent from DMF to non-polar toluene the yield of target product increased to 62% (Table 5, entry 2). Though we are unable to provide a clear answer for this observations but polarity of the solvent is significantly

affecting the kinetics of coupling reaction. Thus, we chose toluene as reaction media for further transformations. The present approach for carrying out Sonogashira coupling is better than the approaches reported in the literature⁴⁰⁻⁴⁶ (Scheme 7). Next, we examined the photocatalytic activity of photocatalysts **DA2-DA4** towards Sonogashira coupling under optimized conditions. In case of **DA2**, the target compound was obtained only in 35% yield (Table 5, entry 3) while with **DA3**

Table 5. Optimization of reactions conditions for Sonogashira coupling between aryl halide and phenylacetylene



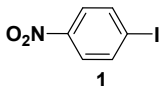
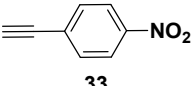
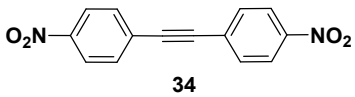
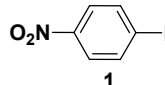
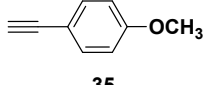
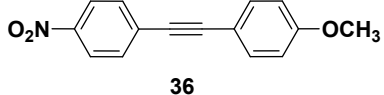
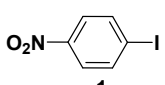
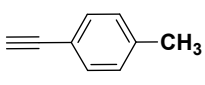
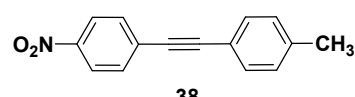
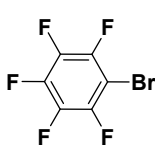
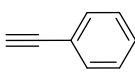
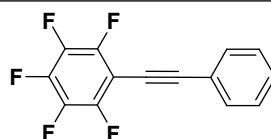
Entry	Photocatalyst	Solvent	Yield
1.	DA1	DMF	40%
2.	DA1	Toluene	62%
3.	DA2	Toluene	35%
4.	DA3	Toluene	20%
5.	DA4	Toluene	15%
6.	-	Toluene	Traces
7.	DA1 ^a	Toluene	Traces
8.	DA1 ^b	Toluene	Traces
a dark, b aerial			

and **DA4** the desired products were obtained in 20% and 15% yields, respectively (Table 5, entries 4 and 5). All the control experiments show that presence of light, inert atmosphere, sacrificial donor and photocatalyst **DA1** are essential for the reaction to proceed in the forward direction. No product

formation was observed in the absence of any of these components (Table 5, entries 6-8).

To understand the reason behind the low catalytic activity of **DA2-DA4**, we examined the reductive quenching of all photocatalysts using TEA as donor. The maximum quenching (90%) of emission was observed in case of **DA1** (Figure S40, SI).

Table 6. The Sonogashira coupling between different aryl halides and different alkyne using photocatalyst **DA1** under optimized

Entry	Aryl halide	Alkyne	Alkyne	Time	Yield%
1.				18 h	63%
2.				18 h	60%
3.				18 h	55%
4.				8 h	60%

On the other hand, in case of derivatives **DA2** and **DA3** 48% and 35% of quenching was observed (Figures S41 and S42, SI), respectively. Further, no significant change in the emission behaviour of **DA4** was observed in the presence of TEA (Figure



1
2
3 S43, SI). We believe that the derivative **DA1** shows good
4
5 catalytic efficiency in Sonogashira coupling due to its high
6
7 ability to accept the electron from triethylamine in the excited
8
9 state to generate radical anion.
10
11
12
13
14
15
16
17
18
19
20
21
22
23
24
25
26
27
28
29
30
31
32
33
34
35
36
37
38

39 With optimized conditions in hand, we examined the substrate
40
41 scope with regard to alkynes. The electron rich/electron
42
43 deficient alkynes furnished the desired products in good yield
44
45 (Table 6, entries 1-3).
46
47

48 Next, we checked the substrate scope with respect to aryl
49
50 halides and it was found only activated aryl halides (electron
51
52 deficient) furnished the desired product (Table 6, entry 4). As
53
54 discussed earlier, iodobenzene or electron rich aryl halide
55
56
57
58
59
60

could not couple with alkyne in presence of **DA1** as photocatalyst due to its high reduction potential.

To get insight into the reaction mechanism, we carried out model reaction in the presence of radical scavenger TEMPO (1.0 equiv.) (Scheme 8a) The desired product was obtained in traces under optimized reaction conditions after 24 h, however, we detected the formation of adduct between 4-nitrobenzene and TEMPO by mass spectrometric analysis (Figure S44, SI). This study suggests the formation of aryl radical in the reaction mixture. Further, the GC-MS spectrum of reaction mixture of model reaction shows the peak corresponding to 1-nitro-4-styrylbenzene ($m/z = 225.25$) which supports the formation of alkene as side product (Figure S45, SI). Based on these experimental observations, we propose the reaction mechanism as shown in scheme 8b. The **DA1** accepts the electron from sacrificial donor and photoreductant **DA1**^{•-} have sufficient reduction potential to activate aryl halide 'A' to generates radical anion 'B'. The intermediate 'B' then undergoes cleavage to generate aryl radical 'C' which further reacts with phenylacetylene in the presence of amino radical of triethylamine to form desired product 'D'.

3. Conclusion

We designed and synthesized donor acceptor systems **DA1-DA4** which absorb strongly in visible region and show systematically elevated reductive potential (-1.25 to -1.71 V) with a gradual decrease in their HOMO-LUMO gap upon increasing the donor

strength. Among all the derivatives, derivative **DA2** exhibits high catalytic activity in C-N bond formation reactions. Despite the high ground state reduction potential, the derivative **DA4** shows low catalytic activity. In case highly activated aryl halide energy as well as electron transfer pathway is proposed whereas in case of other aryl halide such as bromobenzonitrile, 3,5-difluoro bromobenzene electron transfer route is proposed. Very interestingly, derivative **DA1** shows catalytic efficiency in 'metal free' Sonogashira coupling reaction involving activated aryl halides due to its high excited state reduction potential.

4. Experimental Section

4.1 General Experimental Methods and Materials⁴⁷

'All the reagents were purchased from Aldrich and were used without further purification. HPLC grade solvents were used in UV-vis and fluorescence studies. UV-vis spectra were recorded on a SHIMADZU UV-2450 spectrophotometer, with a quartz cuvette (path length 1 cm). The fluorescence spectra were recorded with a HORIBA Scientific FluoroMax-4 spectrofluorometer. The quantum yields were calculated using integrated spheres. The time-resolved fluorescence spectra were recorded with a HORIBA time-resolved fluorescence spectrometer. The electrochemical measurements were performed at room temperature using a computer controlled potentiostat/galvanostat Autolab PGSTAT204 (Netherlands) Metrohm, equipped with FRA (frequency response

analyzer) module. The NOVA software was used to collect, plot and analyze the raw data of various CV measurements. The computational studies were performed using Gaussian 09. ^1H and ^{13}C NMR spectra were recorded on Bruker Avance III HD 500 MHz and JEOL-FT NMR-AL 400 MHz spectrophotometers using $\text{CDCl}_3/\text{DMSO}-d_6$ as solvents and tetramethylsilane, SiMe_4 as internal standards. Data are reported as follows: chemical shift in ppm (d), multiplicity (s = singlet, d = doublet, t = triplet, m = multiplet, br = broad singlet), coupling constants J (Hz).'

4.2 UV-vis and fluorescence studies

The stock solution (10^{-3} M) of **DA1/DA2/DA3/DA4** derivative was prepared by dissolving 4.92 mg/6.10 mg/8.35/6.14 mg of the respective compound in 10.0 mL of DMF. 15.0 μL of this stock solution was further diluted with 2985 μL of DMF/toluene to prepare 3.0 mL solutions of derivatives (5.0 μM). These solutions were used for each UV-vis and fluorescence experiments.

4.3 Synthesis of **A1**²⁶

A solution of phenanthrene-9,10-dione (0.4 g, 1.923 mmol) and 4,5-dibromobenzene-1,2-diamine (0.5g, 1.923 mmol) in 20 ml acetic acid was refluxed at 90 $^\circ\text{C}$ (oil bath) for 12 h (Scheme S1, SI). After completion of the reaction, it was allowed to cool to room temperature. Upon cooling yellow colored precipitates were formed which were filtered and washed with

methanol to give 710 mg (85%) of compound **A1** as dark yellow powder with mp > 250 °C (Reported in literature mp > 250 °C).²⁶

4.4 Synthesis of phenazine based donor acceptor system **DA1**

To a solution of 11,12-dibromodibenzo[a,c]phenazine, **A1** (0.4 g, 0.909 mmol) and 4-methoxy phenylboronic acid **D1** (0.5g, 2.27 mmol) in 20 ml of dioxane, was added 2.0 ml aqueous solution of K₂CO₃ (1.0g, 7.72 mmol) followed by addition of Pd(PPh₃)₄ (0.383g, 0.545 mmol) as a catalyst under N₂ atm (Scheme S2, SI). The reaction mixture was refluxed (oil bath) overnight and thereafter cooled to room temperature and was treated with water. The aqueous layer was extracted with ethyl acetate (3×10 ml), and the combined organic layer was dried over anhydrous sodium sulphate and then distilled under reduced pressure to give a solid residue. The desired product was isolated by column chromatography using ethyl acetate/hexane (20/80) as an eluent. Finally the product was recrystallized from methanol to obtain 361 mg (80%) of derivative **DA1** as light green solid ; mp: >280 °C; ¹H NMR (400 MHz, CDCl₃): δ (ppm) = 9.40 (d, *J* = 8Hz, 2H, Ar-H), 8.58 (d, *J* = 8Hz, 2H, Ar-H), 8.32 (s, 2H), 7.82-7.73 (m, 4H, Ar-H), 7.27-7.24 (m, 4H, Ar-H), 6.86 (d, *J* = 8Hz, 4H, Ar-H), 3.84 (s, 6H, OCH₃), ¹³C{¹H} NMR (CDCl₃, 100 MHz,) δ (ppm) = 158.9, 143.2, 142.6, 141.5, 133.1, 132.0, 131.2, 130.3, 130.1, 128.00, 126.3, 123.0, 113.6, 55.4; HRMS (ESI) *m/z* [M + H]⁺ calcd for C₃₄H₂₅N₂O₂ 493.1916, found 493.1399; Elemental Analysis of **DA1**

for $C_{34}H_{24}N_2O_2$: calculated C, 82.91; H, 4.91; N, 5.69; found: C, 82.51; H, 4.97; N, 5.47 (Figures S70–72, SI).

4.5 General procedure for the synthesis of phenazine based donor acceptor systems DA2/DA3/DA4

A solution of 11,12-dibromodibenzo[a,c]phenazine, **A1** (0.25 g, 0.570 mmol), carbazole (**D2**) (0.20 g, 1.255 mmol)/ 3,6-di-tert-butylcarbazole (**D3**) (0.35g, 1.255 mmol)/ diphenylamine (**D4**) (0.212 g, 1.255 mmol) and K_2CO_3 (0.31 g, 2.28 mmol) in 8 ml of dry nitrobenzene was stirred under nitrogen for 30 min. The reaction mixture was degassed three times and then CuI (0.13 g, 0.2 mmol) was introduced followed by addition of 18-C-6 in catalytic amount under inert atmosphere (Schemes S3-S5, SI). The reaction mixture was refluxed at 200 °C (sand bath) for 48 h under nitrogen. After completion of the reaction (TLC), the reaction mixture was treated with water. The aqueous layer was extracted with ethyl acetate (3×10 ml). The combined organic layer was dried over anhydrous sodium sulphate and then distilled under reduced pressure to give a solid residue. The desired product was isolated by column chromatography using ethyl acetate/hexane (5/95) as an eluent and finally the product was recrystallized from methanol to give **DA2/DA3/DA4** in 245 (70%)/355 (70%)/280 (80%) mg.

Characterization of DA2: Yellow solid ; mp: >280 °C; 1H NMR (500 MHz, DMSO- d_6): δ (ppm) = 9.33 (dd, J = 17.5Hz, 4H, Ar-H), 8.82 (d, J = 10Hz, 2H, Ar-H), 8.60 (d, J = 10Hz, 2H, Ar-H), 8.55 (s, 2H), 8.31 (d, J = 5Hz, 2H, Ar-H), 8.28-8.24 (m, 2H, Ar-H), 7.92 (q, J = 10Hz, 3H, Ar-H), 7.87-7.80 (m, 3H, Ar-H), 7.67 (d, J = 10Hz, 2H, Ar-H), 7.50 (t, J = 7.5Hz, 2H, Ar-H), 7.37 (t, J = 7.5Hz, 2H, Ar-H), $^{13}C\{^1H\}$ NMR (DMSO- d_6 /CDCl $_3$; 8/2, 100 MHz,) δ (ppm) = 140.2, 138.7, 138.1, 136.7, 129.8, 129.2, 127.5, 126.5, 124.7, 124.1, 123.9, 123.2, 121.8, 121.45, 118.9, 118.8, 112.2, 108.00, 106.9; HRMS (ESI) m/z $[M+H]^+$ calcd for $C_{44}H_{27}N_4$ 611.2236,

found 611.2238; Elemental Analysis of **DA2** for $C_{44}H_{26}N_4$: calculated C, 86.53; H, 4.29; N, 9.17; found: C, 86.48; H, 4.26; N, 9.11 (Figures S73-75, SI).

Characterization of DA3: Dark yellow solid ; mp: >280 °C; 1H NMR (400 MHz, $CDCl_3$): δ (ppm) = 9.44 (dd, J = 14Hz, 4H, Ar-H), 8.61 (d, J = 4Hz, 2H, Ar-H), 8.54 (s, 2H), 8.51 (d, J = 8Hz, 1H, Ar-H), 8.20 (s, 2H), 8.13 (d, J = 4Hz, 1H, Ar-H), 7.85-7.80 (m, 3H, Ar-H), 7.79-7.75 (m, 3H, Ar-H), 7.63 (d, J = 4Hz, 2H, Ar-H), 7.53 (d, J = 8Hz, 2H, Ar-H), 1.50 (s, 36H, CH_3), $^{13}C\{^1H\}$ NMR ($CDCl_3$, 100 MHz,) δ (ppm) = 143.7, 143.0, 142.8, 142.4, 140.8, 139.3, 138.8, 132.0, 130.9, 130.5, 130.4, 130.1, 128.7, 128.0, 126.2, 124.8, 123.9, 122.0, 116.4, 109.4, 34.8, 32.00; HRMS (ESI) m/z $[M + Na]^+$ calcd for $C_{60}H_{58}N_4Na$ 858.1418, found 858.1443; Elemental Analysis of **DA3** for $C_{60}H_{58}N_4$: calculated C, 86.29; H, 7.00; N, 6.71; found: C, 86.24; H, 6.66; N, 6.40 (Figures S76-78, SI).

Characterization of DA4: Orange solid; mp: >280 °C; 1H NMR (400 MHz, $CDCl_3$): δ (ppm) = 9.34 (d, J = 10Hz, 1H, Ar-H), 9.27 (d, J = 10Hz, 1H, Ar-H), 8.56 (d, J = 10Hz, 2H), 8.11 (d, J = 10Hz, 1H, Ar-H), 7.78-7.64 (m, 8H, Ar-H), 7.39-7.36 (m, 5H, Ar-H), 7.28-7.17 (m, 12H, Ar-H), $^{13}C\{^1H\}$ NMR ($CDCl_3$, 100 MHz,) δ (ppm) = 147.0, 132.1, 130.4, 130.1, 129.8, 129.6, 129.4, 127.9, 127.8, 127.2, 127.0, 126.2, 125.9, 125.7, 124.7, 124.4, 122.9, 116.4; HRMS (ESI) m/z $[M+H]^+$ calcd for $C_{44}H_{31}N_4$ 615.2549, found 615.2549; Elemental Analysis of **DA4** for $C_{44}H_{30}N_4$: calculated C, 85.97; H, 4.92; N, 9.11; found: C, 85.80; H, 4.93; N, 8.99 (Figures S79-81, SI).

4.6 General procedure for photocatalytic C-N cross coupling catalyzed by donor acceptor (DA) systems.

A mixture of aryl halide (1.0 mmol) and **DA** (0.1 mol%) in DMF (2.0 ml) was degassed three times. Next, the amine (5.0 mmol)

was introduced to the reaction mixture in the presence of nitrogen. The reaction mixture was stirred for 3-12 h at 40 °C (oil bath) under irradiation with white LED (16 W). After the completion of the reaction (monitored by TLC), the reaction mixture was cooled to room temperature and treated with water. The aqueous layer was extracted with ethyl acetate. The combined organic layer was dried over anhydrous sodium sulphate and distilled under reduced pressure to furnish a solid residue. The desired products were obtained by recrystallization from methanol:ethylacetate (5:1) mixture except **20**, **21**, **22**, **25**, **28** and **29** which were purified by column chromatography using ethyl acetate/hexane as an eluent followed by recrystallization from methanol (Figures S46-S64, SI).

4.7 General procedure for Photocatalytic Sonogashira coupling catalyzed by donor acceptor (DA) systems.

A mixture of aryl halide (1.0 mmol), alkyne (1.0 mmol) and **DA** photocatalyst (0.1 mol%) in toluene (2.0 ml) was degassed three times. Next, triethylamine (5.0 mmol) was introduced to the reaction mixture under inert atmosphere. The reaction mixture was stirred for 8-18 h at 40 °C (oil bath) temperature under irradiation with white LED (16 W). After the completion of the reaction (TLC), the reaction mixture was cooled to room temperature and it was extracted using ethyl acetate (3×10 ml). The combined organic layer was dried over anhydrous sodium

1
2
3 sulphate and distilled under reduced pressure to furnish a solid
4
5 residue. The desired products (**32**, **34**, **36**, **38** and **39**) were
6
7 obtained by column chromatography using hexane as an eluent.
8
9 Finally, all the products were recrystallized using methanol as
10
11 solvent (Figures S65-69, SI).
12
13
14
15

16 17 **4.8 ¹H NMR Characterization of Catalytic Products**

18
19 **1-(4-nitrophenyl)pyrrolidine (3)**⁴⁸ Yellow solid, 176 mg; 92% yield ¹H NMR (500 MHz,
20
21 CDCl₃): δ (ppm) = 8.12 (d, *J* = 10 Hz, 2H, Ar-H), 6.47 (d, *J* = 10 Hz, 2H, Ar-H), 3.41 (t, *J* = 4
22
23 Hz, 4H, CH₂), 2.09-2.05 (m, 4H, CH₂).
24

25
26 **1-(4-Nitrophenyl)piperidine (5)**⁴⁸ yellow oil, 187 mg; 91% yield. ¹H NMR (500 MHz, CDCl₃):
27
28 δ (ppm) = 8.10 (d, *J* = 10 Hz, 2H, Ar-H), 6.79 (d, *J* = 10 Hz, 2H, Ar-H), 3.45 (t, *J* = 5 Hz, 4H,
29
30 CH₂), 1.69-1.67 (m, 6H, CH₂).
31

32
33 **4-(4-Nitrophenyl)morpholine (7)**⁴⁸ yellow solid, 156 mg; 75% yield. ¹H NMR (500 MHz,
34
35 CDCl₃): δ (ppm) = 8.15 (d, *J* = 10 Hz, 2H, Ar-H), 6.84 (d, *J* = 10 Hz, 2H, Ar-H), 3.87 (t, *J* = 5
36
37 Hz, 4H, CH₂), 3.38 (t, *J* = 5 Hz, 4H, CH₂).
38

39
40 ***N*-butyl-4-nitroaniline (9)**⁴⁹ yellow solid, 159 mg; 82% yield. ¹H NMR (500 MHz, CDCl₃): δ
41
42 (ppm) = 8.08 (d, *J* = 10 Hz, 2H, Ar-H), 6.51 (d, *J* = 10 Hz, 2H, Ar-H), 4.46 (s, br, 1H, NH), 3.21
43
44 (q, *J* = 15 Hz, 2H, CH₂), 1.67-1.61 (m, 2H, CH₂), 1.48-1.41 (m, 2H, CH₂), 0.98 (t, *J* = 7.5 Hz,
45
46 3H, CH₃).
47

48
49 ***N,N*-dimethyl-4-nitroaniline (11)**⁵⁰ yellow crystalline solid, 146 mg; 88% yield. ¹H NMR (500
50
51 MHz, CDCl₃): δ (ppm) = 8.13 (d, *J* = 10 Hz, 2H, Ar-H), 6.61 (d, *J* = 10 Hz, 2H, Ar-H), 3.11 (s,
52
53 6H, CH₃).
54
55
56
57
58
59
60

4-nitroaniline (13)⁴⁸ yellow solid, 124 mg; 90% yield. ¹H NMR (500 MHz, CDCl₃): δ (ppm) = 8.07 (d, *J* = 10 Hz, 2H, Ar-H), 6.63 (d, *J* = 10 Hz, 2H, Ar-H), 4.40 (s, 2H, NH).

***N*-Phenyl-4-nitroaniline (15)**⁴⁸ yellow solid, 145 mg; 68% yield. ¹H NMR (500 MHz, CDCl₃): δ (ppm) = 8.12 (d, *J* = 10 Hz, 2H, Ar-H), 7.39 (t, *J* = 7.5 Hz, 2H, Ar-H), 7.21 (d, *J* = 10 Hz, 2H, Ar-H), 7.17 (t, *J* = 7.5 Hz, 1H, Ar-H), 6.94 (d, *J* = 10 Hz, 2H, Ar-H), 6.26 (s, br, 1H, NH).

4-(pyrrolidin-1-yl)benzonitrile (20)¹³ white solid, 129 mg; 75% yield. ¹H NMR (400 MHz, CDCl₃): δ (ppm) = 7.44 (d, *J* = 8 Hz, 2H, Ar-H), 6.49 (d, *J* = 10 Hz, 2H, Ar-H), 3.32 (t, *J* = 4 Hz, 4H, CH₂), 2.06-2.02 (m, 4H, CH₂).

4-(piperidin-1-yl)benzonitrile (21)⁵¹ white solid, 133 mg; 72% yield. ¹H NMR (400 MHz, CDCl₃): δ (ppm) = 7.46 (d, *J* = 8 Hz, 2H, Ar-H), 6.84 (d, *J* = 8 Hz, 2H, Ar-H), 3.32 (t, *J* = 4 Hz, 4H, CH₂), 1.66-1.60 (m, 6H, CH₂).

4-Morpholin-4-ylbenzonitrile (22)⁴⁸ white solid, 112 mg; 60% yield. ¹H NMR (400 MHz, CDCl₃): δ (ppm) = 7.74 (d, *J* = 8 Hz, 2H, Ar-H), 6.89 (d, *J* = 8 Hz, 2H, Ar-H), 3.86 (t, *J* = 4 Hz, 4H, CH₂), 3.27 (t, *J* = 6 Hz, 4H, CH₂).

1-(perfluorophenyl)pyrrolidine (24)⁵¹ yellow oil, 220 mg; 93% yield. ¹H NMR (400 MHz, CDCl₃): δ (ppm) = 3.59 (t, *J* = 6 Hz, 4H, CH₂), 1.95-1.88 (m, 4H, CH₂).

1-(perfluorophenyl)piperidine (25)⁵¹ yellow oil, 220 mg; 90% yield. ¹H NMR (500 MHz, CDCl₃): δ (ppm) = 3.18 (t, *J* = 5 Hz, 4H, CH₂), 1.68-1.65 (m, 4H, CH₂), 1.62-1.58 (m, 2H, CH₂).

4-(perfluorophenyl)morpholine (26)⁵¹ white solid 207 mg; 82% yield. ¹H NMR (400 MHz, CDCl₃): δ (ppm) = 3.81 (t, *J* = 4 Hz, 4H, CH₂), 3.27-3.25 (m, *J* = 4 Hz, 4H, CH₂).

1-(3,5-difluorophenyl)pyrrolidine (28) yellow oil, 150 mg; 82% yield. ¹H NMR (400 MHz, CDCl₃): δ (ppm) = 6.50 (tt, 1H, Ar-H), 6.44-6.43 (m, 1H, Ar-H), 6.14 (tt, 1H, Ar-H), 3.23 (t, *J* = 6 Hz, 4H, CH₂), 2.02-1.99 (m, 4H, CH₂); ¹³C{¹H} NMR (CDCl₃, 100 MHz,) δ (ppm) =

146.8, 122.8, 110.3, 105.3, 97.4, 47.7, 25.4; HRMS (ESI) m/z $[M + K]^+$ calcd for $C_{10}H_{11}F_2NK$ 222.0497, found 222.1118.

1-(3,5-difluorophenyl)piperidine (29) yellow oil, 157 mg; 80% yield. 1H NMR (400 MHz, $CDCl_3$): δ (ppm) = 6.79-6.78 (m, 1H, Ar-H), 6.62 (tt, 1H, Ar-H), 6.49 (tt, 1H, Ar-H), 3.17 (t, J = 6Hz, 4H, CH_2), 1.69-1.64 (m, 4H, CH_2), 1.61-1.57 (m, 2H, CH_2); HRMS (ESI) m/z $[M + H]^+$ calcd for $C_{11}H_{14}F_2N$ 198.1094, found 198.1845.

4-(3,5-difluorophenyl)morpholine (30)¹² white solid, 129 mg; 65% yield. 1H NMR (400 MHz, $CDCl_3$): δ (ppm) = 6.79-6.78 (m, 1H, Ar-H), 6.72 (tt, 1H, Ar-H), 6.50 (tt, 1H, Ar-H), 3.83 (t, J = 4Hz, 4H, CH_2), 3.15 (t, J = 4Hz, 4H, CH_2).

1-nitro-4-(phenylethynyl)benzene (32)⁵² light yellow solid, 138 mg; 62% yield. 1H NMR (400 MHz, $CDCl_3$): δ (ppm) = 8.22 (d, J = 8 Hz, 2H), 7.67 (d, J = 8 Hz, 2H), 7.57-7.55 (m, 2H), 7.40-7.37 (m, 3H).

1,2-bis(4-nitrophenyl)ethyne (34)⁵³ light yellow solid, 162 mg; 63% yield. 1H NMR (400 MHz, $CDCl_3$): δ (ppm) = 8.27 (d, J = 12 Hz, 4H), 7.72 (d, J = 8 Hz, 4H).

1-methoxy-4-(4-nitrophenyl)ethynyl)benzene (36)⁵⁴ light yellow solid, 151 mg; 60% yield. 1H NMR (400 MHz, $CDCl_3$): δ (ppm) = 8.21 (d, J = 8 Hz, 2H), 7.63 (d, J = 8 Hz, 2H), 7.50 (d, J = 8 Hz, 2H), 6.91 (d, J = 8 Hz, 2H), 3.85 (s, 3H, OCH_3).

1-methyl-4-((4-nitrophenyl)ethynyl)benzene (38)⁵⁵ light yellow solid, 130 mg; 55% yield. 1H NMR (400 MHz, $CDCl_3$): δ (ppm) = 8.22 (d, J = 12 Hz, 2H), 7.65 (d, J = 8 Hz, 2H), 7.45 (d, J = 8 Hz, 2H), 7.20 (d, J = 4 Hz, 2H), 2.39 (s, 3H, CH_3).

1,2,3,4,5-pentafluoro-6-(phenylethynyl)benzene (39)⁵⁶ white solid, 160 mg; 60% yield. 1H NMR (400 MHz, $CDCl_3$): δ (ppm) = 7.53 (d, J = 8 Hz, 2H), 7.38-7.32 (m, 3H).

ASSOCIATED CONTENT

Supporting Information. The contents of the SI section include ^1H , ^{13}C and mass spectra of compounds. UV-vis, fluorescence, electrochemical studies and computational data. This material is available free of charge via the Internet at <http://pubs.acs.org>

AUTHOR INFORMATION

Corresponding Author

* E-mail: vanmanan@yahoo.co.in

Notes

Authors declare no competing financial interest.

ACKNOWLEDGMENT

V.B. is thankful SERB, New Delhi (ref. no. CRG/2018/001274), CSIR New Delhi (No. 02(0358/19/EMR-II) and RUSA 2.0 for financial support. H.D. is thankful to UGC-BSR for Senior Research Fellowship (SRF). G.S is thankful to CSIR New Delhi for Senior Research Fellowship (SRF).

REFERENCES

1. Muci, A. R.; Buchwald, S. L. Practical Palladium Catalysts for C-N and C-O Bond Formation. *Cross-Coupling React.* **2002**, *219*, 131-209.

2. Stump, B.; Eberle, C.; Kaiser, M.; Brun, R.; Krauth-Siegel, R. L.; Diederich, F. Diaryl Sulfide-Based Inhibitors of Trypanothione Reductase: Inhibition Potency, Revised Binding Mode and Antiprotozoal Activities. *Org. Biomol. Chem.* **2008**, *6*, 3935-3947.

3. Cao, X.-T.; Zhang, P.-F.; Zheng, H. Metal-Free Catalytic Synthesis of Diaryl Thioethers Under Mild Conditions. *New J. Chem.* **2016**, *40*, 6762-6767.

4. Ruiz-Castillo, P.; Buchwald, S. L. Applications of Palladium-Catalyzed C-N Cross-Coupling Reactions. *Chem. Rev.* **2016**, *116*, 12564-12649.

5. Shekarrao, K.; Kaishap, P. P.; Gogoi, S.; Boruaha, R. C. Palladium-Catalyzed One-Pot Sonogashira Coupling, exo-dig Cyclization and Hydride Transfer Reaction: Synthesis of Pyridine-Substituted Pyrroles. *Adv. Synth. Catal.* **2015**, *357*, 1187-1192.

6. Paul, F.; Patt, J.; Hartwig, J. Palladium-Catalyzed Formation of Carbon-Nitrogen Bonds. Reaction Intermediates and Catalyst Improvements in the Hetero Cross-Coupling of Aryl Halides and Tin Amides. *J. Am. Chem. Soc.* **1994**, *116*, 5969-5970.

7. Chinchilla, R.; Najera, C. Recent Advances in Sonogashira Reactions. *Chem. Soc. Rev.* **2011**, *40*, 5084-5121.

8. Beletskaya, I. P.; Cheprakov, A. V. Copper in Cross-Coupling Reactions: The post-Ullmann Chemistry. *Coord. Chem. Rev.* **2004**, *248*, 2337-2364.

9. Ley, S. V.; Thomas, A. W. Modern Synthetic Methods for Copper-Mediated C(aryl)-O, C(aryl)-N, and C(aryl)-S Bond Formation. *Angew. Chem., Int. Ed.* **2003**, *42*, 5400-5449.

10. Yoo, W.-J.; Tsukamoto, T.; Kobayashi, S. Visible Light-Mediated Ullmann-Type C-N Coupling Reactions of Carbazole Derivatives and Aryl Iodides. *Org. Lett.* **2015**, *17*, 3640-3642.

11. Corcoran, E. B.; Pirnot, M. T.; Lin, S.; Dreher, S. D.; Di Rocco, D. A.; Davies, I. W.; Buchwald, S. L.; MacMillan, D. W. C. Aryl Amination Using Ligand-Free Ni(II) Salts and Photoredox Catalysis. *Science* **2016**, *353*, 279-283.

12. Du, Y.; Pearson, R. M.; Lim, C.-H.; Sartor, S. M.; Ryan, M. D.; Yang, H.; Damrauer, N. H.; Miyake, G. M. Strongly Reducing, Visible-Light Organic Photoredox Catalysts as Sustainable Alternatives to Precious Metals. *Chem. Eur. J.* **2017**, *23*, 10962 - 10968.

13. Liu, Y.-Y.; Liang, D.; Lu, L.-Q.; Xiao, W.-J. Practical Heterogeneous Photoredox/Nickel Dual Catalysis for C-N and C-O Coupling Reactions. *Chem. Commun.* **2019**, *55*, 4853-4856.

14. Kudisch, M.; Lim, C.-H.; Thordarson, P.; Miyake, G. M. Energy Transfer to Ni-Amine Complexes in Dual Catalytic, Light-Driven C–N Cross-Coupling Reactions. *J. Am. Chem. Soc.* **2019**, *141*, 19479–19486.

15. Lim, C.-H.; Kudisch, M.; Liu, B.; Miyake, G. M. C–N Cross-Coupling via Photoexcitation of Nickel-Amine Complexes. *J. Am. Chem. Soc.* **2018**, *140*, 7667–7673.

16. Ghosh, I.; Khamrai, J.; Savateev, A.; Shlapakov, N.; Antonietti, M.; König, B. Organic Semiconductor Photocatalyst can Bifunctionalize Arenes and Heteroarenes. *Science* **2019**, *365*, 360–366.

17. Dadwal, S.; Deol, H.; Kumar, M.; Bhalla, V. AIEE Active Nanoassemblies of Pyrazine Based Organic Photosensitizers as Efficient Metal-Free Supramolecular Photoredox Catalytic Systems. *Sci. Rep.* **2019**, *9*, 11142.

18. Neumann, M.; Fuldner, S.; König, B.; Zeitler, K. Metal-Free, Cooperative Asymmetric Organophotoredox Catalysis with Visible Light. *Angew. Chem. Int. Ed.* **2011**, *50*, 951–954.

19. Ghosh, I.; Marzo, L.; Das, A.; Shaikh, R.; König, B. Visible Light Mediated Photoredox Catalytic Arylation Reactions. *Acc. Chem. Res.* **2016**, *49*, 1566–1577.

20. Singh, V. K.; Yu, C.; Badgujar, S.; Kim, Y.; Kwon, Y.; Kim, D.; Lee, J.; Akhter, T.; Thangavel, G.; Park, L. S.; Lee, J.;

Nandajan, P. C.; Wannemacher, R.; Milián-Medina, B.; Lüler, L.; Kim, K. S.; Gierschner, J.; Kwon, M. S. Highly Efficient Organic Photocatalysts Discovered via a Computer-Aided-Design Strategy for Visible-Light-Driven Atom Transfer Radical Polymerization. *Nat. Catal.* **2018**, *1*, 794-804.

21. Speckmeier, E.; Fischer, T. G.; Zeitler, K. A Toolbox Approach to Construct Broadly Applicable Metal-Free Catalysts for Photoredox Chemistry: Deliberate Tuning of Redox Potentials and Importance of Halogens in Donor-Acceptor Cyanoarenes. *J. Am. Chem. Soc.* **2018**, *140*, 15353-15365.

22. Liu, M.; Gao, Y.; Zhang, Y.; Liu, Z.; Zhao, L. Quinoxaline-Based Conjugated Polymers for Polymer Solar Cells. *Polymer. Chem.* **2017**, *8*, 4613-4636.

23. Zhang, Y.; Zou, J.; Yip, H.-L.; Chen, K.-S.; Zeigler, D. F.; Sun, Y.; Jen, A. K.-Y. Indacenodithiophene and Quinoxaline-Based Conjugated Polymers for Highly Efficient Polymer Solar Cells. *Chem. Mater.* **2011**, *23*, 2289-2291.

24. Data, P.; Pander, P.; Okazaki, M.; Takeda, Y.; Minakata, S.; Monkman, A. P. Dibenzo[a,j]phenazine-Cored Donor-Acceptor-Donor Compounds as Green-to-Red/NIR Thermally Activated Delayed Fluorescence Organic Light Emitters. *Angew. Chem. Int. Ed.* **2016**, *55*, 5739-5744.

25. Furue, R.; Matsuo, K.; Ashikari, Y.; Ooka, H.; Amanokura, N.; Yasuda, T. Highly Efficient Red-Orange Delayed Fluorescence Emitters Based on Strong π -Accepting Dibenzophenazine and Dibenzoquinoxaline Cores: Toward a Rational Pure-Red OLED Design. *Adv. Optical Mater.* **2018**, *6*, 1701147.

26. Putta, A.; Mottishaw, J. D.; Wang, Z.; Sun, H. Rational Design of Lamellar π - π Stacked Organic Crystalline Materials with Short Interplanar Distance. *Cryst. Growth Des.* **2014**, *14*, 350-356.

27. Buzzetti, L.; Crisenza, G. E. M.; Melchiorre, P. Mechanistic Studies in Photocatalysis. *Angew. Chem. Int. Ed.* **2019**, *58*, 3730-3747.

28. S. D.-M.; Islam, Konishi, T.; Fujitsuka, M.; Ito, O.; Nakamura, Y.; Usui, Y. Photosensitized Reduction of Methyl Viologen Using Eosin-Y in Presence of a Sacrificial Electron Donor in Water-Alcohol Mixture *Photochem. Photobiol.* **2000**, *71*, 675-680.

29. Martindale, B. C. M.; Hutton, G. A. M.; Caputo, C. A.; Reisner, E. Solar Hydrogen Production Using Carbon Quantum Dots and a Molecular Nickel Catalyst. *J. Am. Chem. Soc.* **2015**, *137*, 6018-6025.

30. Yong, W.-W.; Lu, H.; Li, H.; Wang, S.; Zhang, M.-T. Photocatalytic Hydrogen Production with Conjugated Polymers as Photosensitizers. *ACS Appl. Mater. Interfaces* **2018**, *10*, 10828-10834.

31. Costentin, C.; Robert, M.; Saveant, J.-M. Fragmentation of Aryl Halide π Anion Radicals. Bending of the Cleaving Bond and Activation vs Driving Force Relationships. *J. Am. Chem. Soc.* **2004**, *126*, 16051-16057.

32. Pause, L.; Robert, M.; Saveant, J.-M. Can Single-Electron Transfer Break an Aromatic Carbon-Heteroatom Bond in One Step? A Novel Example of Transition between Stepwise and Concerted Mechanisms in the Reduction of Aromatic Iodides. *J. Am. Chem. Soc.* **1999**, *121*, 7158-7159.

33. Ghosh, I.; Shaikh, R. S.; König, B. Sensitization-Initiated Electron Transfer for Photoredox Catalysis. *Angew. Chem. Int. Ed.* **2017**, *56*, 8544-8549.

34. Lima, C. G. S.; Lima, T. de M.; Duarte, M.; Jurberg, I. D.; Paixão, M. W. Organic Synthesis Enabled by Light-Irradiation of EDA Complexes: Theoretical Background and Synthetic Applications. *ACS Catal.* **2016**, *6*, 3, 1389-1407.

35. Buzzetti, L.; Crisenza, G. E. M.; Melchiorre, P. Mechanistic Studies in Photocatalysis. *Angew. Chem., Int. Ed.* **2019**, *58*, 3730-3747.

36. Ghosh, I.; König, B. Chromoselective Photocatalysis: Controlled Bond Activation through Light-Color Regulation of Redox Potentials. *Angew. Chem. Int. Ed.* **2016**, *55*, 7676-7679.

37. Ghosh, I.; Ghosh, T.; Bardagi, J. I.; König, B. Reduction of Aryl Halides by Consecutive Visible Light-Induced Electron Transfer Processes. *Science* **2014**, 346, 725-728.

38. Meyer, A. U.; Slanina, T.; Yao, C.-J.; König, B. Metal-Free Perfluoroarylation by Visible Light Photoredox Catalysis. *ACS Catal.* **2016**, 6, 369-375.

39. Zhao, Y.; Zhang, C.; Chin, K. F.; Pytela, O.; Wei, G.; Liu, H.; Bureš, F.; Jiang, Z. Dicyanopyrazine-Derived Push-Pull Chromophores for Highly Efficient Photoredox Catalysis. *RSC Adv.* **2014**, 4, 30062-30067.

40. Okuro, K.; Furuune, M.; Enna, M.; Miura, M.; Nomura, M. Synthesis of Aryl- and Vinylacetylene Derivatives by Copper-Catalyzed Reaction of Aryl and Vinyl Iodides with Terminal Alkynes. *J. Org. Chem.* **1993**, 58, 4716-4721.

41. Li, J.-H.; Li, J.-L.; Wang, D.-P.; Pi, S.-F.; Xie, Y.-X.; Zhang, M.-B.; Hu, X. C. CuI-Catalyzed Suzuki-Miyaura and Sonogashira Cross-Coupling Reactions Using DABCO as Ligand. *J. Org. Chem.* **2007**, 72, 2053-2057.

42. Monnier, F.; Turtaut, F. O.; Duroure, L.; Taillefer, M. Copper-Catalyzed Sonogashira-Type Reactions under Mild Palladium-Free Conditions. *Org. Lett.* **2008**, 10, 3203-3206.

43. Saejueng, P.; Bates, C. G.; Venkataraman, D. Copper(I)-Catalyzed Coupling of Terminal Acetylenes with Aryl or Vinyl Halides. *Synthesis* **2005**, *10*, 1706-1712.

44. Zuidema, E.; Bolm, C. Sub-Mol % Catalyst Loading and Ligand-Acceleration in the Copper-Catalyzed Coupling of Aryl Iodides and Terminal Alkyenes. *Chem.-Eur. J.* **2010**, *16*, 4181-4185.

45. Protti, S.; Fagnoni, M.; Albini, A. Photo-Cross-Coupling Reaction of Electron-Rich Aryl Chlorides and Aryl Esters with Alkynes: A Metal-Free Alkynylation. *Angew. Chem. Int. Ed.* **2005**, *44*, 5675-5678.

46. Leadbeater, N. E.; Marco, M.; Tominack, B. J. First Examples of Transition-Metal Free Sonogashira-Type Couplings. *Org. Lett.* **2003**, *5*, 3919-3922.

47. S. Pramanik, V. Bhalla, M. Kumar. Hexaphenylbenzene-Based Fluorescent Aggregates for Ratiometric Detection of Cyanide Ions at Nanomolar Level: Set-Reset Memorized Sequential Logic Device. *ACS Appl. Mater. Interfaces* **2014**, *6*, 5930-5939.

48. Singh, G.; Kumar, M.; Bhalla, V. Ultrafine Hybrid Cu₂O-Fe₂O₃ Nanoparticles Stabilized by Hexaphenylbenzene-Based Supramolecular Assemblies: A Photocatalytic System for the Ullmann-Goldberg Coupling Reaction. *Green Chem.* **2018**, *20*, 5346-5357.

49. Deldaele, C.; Evano, G. Room-Temperature Practical Copper-Catalyzed Amination of Aryl Iodides. *Chem Cat Chem* **2016**, *8*, 1319-1328.

50. Garcia, J.; Sorrentino, J.; Diller, E. J.; Chapman, D.; Woydziak, Z. R. A General Method for Nucleophilic Aromatic Substitution of Aryl Fluorides and Chlorides with Dimethylamine using Hydroxide-Assisted Decomposition of N,N-Dimethylformamide. *Synth Commun.* **2016**, *46*, 475-481.

51. Ge, W.-Z.; Wu, B.-M.; Huang, W.-Y. Nucleophilic Substitution Reaction in Polyfluoroaromatics: I. Reactions with Secondary Amine Nucleophiles. *Ac& Chimicu. Sinicu.* **1984**, *43*, 349-355.

52. Deol, H.; Pramanik, S.; Kumar, M.; Khan, I. A.; Bhalla, V. Supramolecular Ensemble of a TICT-AIEE Active Pyrazine Derivative and CuO NPs: A Potential Photocatalytic System for Sonogashira Couplings. *ACS Catal.* **2016**, *6*, 3771-3783.

53. Ravera, M.; Amato, R. D.; Guerri, A. Probing Delocalisation Across Highly Ethynylated Mono and Dinuclear Pt(II) Tethers Containing Nitro Groups and Organic Models as Redox Active Probes: X-ray Crystal Structure of trans-[Pt(CC-C₆H₄NO₂)₂(PPh₃)₂] *J. Organomet. Chem.* **2005**, *690*, 2376-2380.

54. Hu, H.; Yang, F.; Wu, Y. Palladacycle-Catalyzed Deacetonative Sonogashira Coupling of Aryl Propargyl Alcohols with Aryl Chlorides. *J. Org. Chem.* **2013**, *78*, 10506-10507.

55. Gholap, A. R.; Venkatesan, K.; Pasricha, R.; Daniel, T.; Lahoti, R. J.; Srinivasan, K. V. Copper- and Ligand-Free Sonogashira Reaction Catalyzed by Pd(0) Nanoparticles at Ambient Conditions under Ultrasound Irradiation. *J. Org. Chem.* **2005**, *70*, 4869-4872.

56. Wei, Y.; Zhao, H.; Kan, J.; Su, W.; Hong, M. Copper-Catalyzed Direct Alkynylation of Electron-Deficient Polyfluoroarenes with Terminal Alkynes Using O₂ as an Oxidant. *J. Am. Chem. Soc.* **2010**, *132*, 2522-2523.

TOC graphics

